Chinese Journal of Aeronautics 24 (2011) 777-788

Contents lists available at ScienceDirect

Chinese Journal of Aeronautics

journal homepage: www.elsevier.com/locate/cja

Robust Hybrid Control for Ballistic Missile Longitudinal Autopilot

WAEL Mohsen Ahmed[a,*], QUAN Quan[a,b]

[a]*Department of Automatic Control, School of Automation Science and Electrical Engineering, Beihang University, Beijing 100191, China*

[b]*State Key Laboratory of Virtual Reality Technology and Systems, Beihang University, Beijing 100191, China*

Received 16 December 2010; revised 24 January 2011; accepted 10 May 2011

Abstract

This paper investigates the boost phase's longitudinal autopilot of a ballistic missile equipped with thrust vector control. The existing longitudinal autopilot employs time-invariant passive resistor-inductor-capacitor (RLC) network compensator as a control strategy, which does not take into account the time-varying missile dynamics. This may cause the closed-loop system instability in the presence of large disturbance and dynamics uncertainty. Therefore, the existing controller should be redesigned to achieve more stable vehicle response. In this paper, based on gain-scheduling adaptive control strategy, two different types of optimal controllers are proposed. The first controller is gain-scheduled optimal tuning-proportional-integral-derivative (PID) with actuator constraints, which supplies better response but requires a priori knowledge of the system dynamics. Moreover, the controller has oscillatory response in the presence of dynamic uncertainty. Taking this into account, gain-scheduled optimal linear quadratic (LQ) in conjunction with optimal tuning-compensator offers the greatest scope for controller improvement in the presence of dynamic uncertainty and large disturbance. The latter controller is tested through various scenarios for the validated nonlinear dynamic flight model of the real ballistic missile system with autopilot exposed to external disturbances.

Keywords: ballistic missiles; attitude control; gain-scheduling; optimal tuning-control; LQ optimal regulators

1. Introduction

This paper investigates the boost phase's longitudinal autopilot of a ballistic missile equipped with thrust vector control. The performance quality of the ballistic missile in the powered flight (boost phase) is generally studied in two distinct, but related phases:

(1) Dynamics of motion around center of gravity (short period dynamics/angular motion control).

(2) The center of gravity dynamics (long period dynamics/flight path control).

Generally, the fundamental aim of the autopilot is to achieve adequate stability and reasonable, rapid and well-damped response to input control demand, with moderate insensitivity to external disturbances. Moreover, there are two basic requirements that must be satisfied by the steering control system of a ballistic missile [1]:

(1) Control the missile satisfactorily during the highly critical period of high aerodynamic pressure that occurs as the missile climbs out of the atmosphere at high velocity.

(2) Steer the missile to the proper cutoff condition.

The automatic flight control system of ballistic missiles generally encounters the following constraints:

(1) Influence of missile elasticity.

(2) Dynamic properties of actuators and instrumentation.

(3) The aerodynamic instability of the airframe.

(4) Sloshing of liquid propellants for missiles with

*Corresponding author. Tel.: +86-15910684701.
E-mail address: waelsoliman@live.com
Foundation items: National Natural Science Foundation of China (60904066); National Basic Research Program of China (2010CB327904); "Weishi" Young Teachers Talent Cultivation Foundation of Beihang University (YWF-11-03-Q-013)

doi: 10.1016/S1000-9361(11)60092-7

liquid engine.

(5) Interaction with guidance.

The problems in missile attitude control design arise because the missile is aerodynamically unstable. Moreover, the inertia effects of instrumentation and actuator introduce further complications. The existing longitudinal autopilot employs time-invariant passive resistor-inductor-capacitor (RLC) network compensator as a control strategy, which does not take into account the time-varying missile dynamics. Therefore, the current controller should be redesigned to achieve more stable vehicle response over a larger disturbance and dynamics uncertainty. A controller that improves damping ratio for large pitch demands in the presence of dynamics uncertainty and large disturbance is desirable.

The basic ideas of research and development of improved longitudinal attitude controller is that, for a non-perturbed ascent trajectory of ballistic missile ("boost trajectory"), there is a trajectory that results from standard predicted values of missile thrust, weight, lift, drag, and that experiences no wind velocity. Consequently, the standard pitch program produces standard time histories of missile position, angle of attack, and velocity, which lead to standard time histories of missile longitudinal dynamics.

For time-varying and/or nonlinear systems, one of the most popular methods is gain-scheduling [2-3]. The strategy includes obtaining linearized dynamic models for the plant at usually finitely operating points, designing a linear time-invariant (LTI) control law ("point design") to satisfy local performance objectives for each point, and then adjusting ("scheduling") the controller gains real time as the operating conditions vary. This approach has been applied successfully [4-8], especially for aircraft and process control problems in many years.

In this paper, two different types of optimal controllers are proposed based on gain-scheduling adaptive control strategy:

(1) Gain-scheduled optimal tuning-proportional-integral-derivative (PID) with actuator constraints.

(2) Gain-scheduled optimal linear quadratic (LQ) in conjunction with optimal tuning-compensator.

By simulations, gain-scheduled optimal tuning-PID with actuator constraints has better response but requires a priori knowledge of the system dynamics. However, the controller has oscillatory response in the presence of dynamic uncertainty.

Moreover, it is found that gain-scheduled reduced order linear-quadratic-Gaussian (LQG) is more divergently unstable than the existing controller. The LQG problem combines the linear quadratic regulator (LQR) with an estimation filter. However, the LQG controller often has lower stability margins, lower gain crossover frequency, and slower response when compared to LQR. The main problem of the LQG solution is its lack of robustness which has resulted in a failure in real experiments [9]. As more realism is added to the plant of the system, the LQG becomes unstable in the presence of model uncertainties.

The robust hybrid control is obtained by designing reduced order LQR in conjunction with optimal tuning-compensator. The reduced order LQR problem is solved without taking into account the actuator dynamics. Moreover, the gain-schedule is considered for two-state feedback by ignoring angle of attack state feedback which has less dynamic effect. The proposed longitudinal controller offers the greatest scope for controller improvement, and guarantees damping ratio $\zeta > 0.7$ with overshoot <10% in the presence of dynamic uncertainty and large disturbance. This approach is tested through various scenarios for the validated nonlinear dynamic flight model of the real ballistic missile system with autopilot exposed to external disturbances.

2. Longitudinal Dynamics of Boost Trajectory

2.1. Longitudinal dynamics

This section demonstrates the longitudinal dynamics of the existing ballistic missile system during the boost trajectory. Fig. 1 shows the missile pitch plane dynamics. Where α is the angle of attack, (°); m the total missile mass, kg; V_M the missile total velocity, m/s; θ and ϑ are the flight path angle and missile pitch angle respectively, (°). For the system under investigation, the missile has four air rudders arranged, as shown in Fig. 2, where δ_i (i=1,2,3,4) is rudder deflection angle.

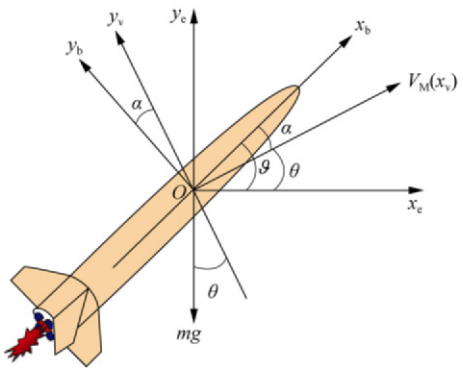

Note: subscript "e"denotes Earth axis, "b" missile body axis, "v" velocity axis.

Fig. 1 Missile pitch plane dynamics.

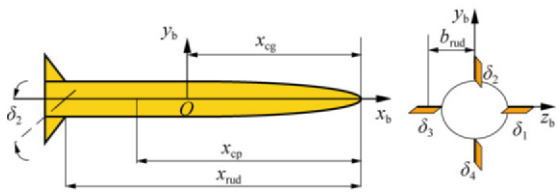

Fig. 2 Air rudder.

For a non-perturbed ascent trajectory ("boost tra-

jectory"), there is a trajectory that results from standard predicted values of missile thrust, weight, lift, drag, and that experiences no wind velocity. Consequently, the standard pitch program produces standard time histories of missile position, angle of attack, and velocity, which lead to standard time histories of missile longitudinal dynamics.

Now we define the control distribution, in which there is air rudder with four control organs as shown in Fig. 2. The control organs 2, 4 are used for pitch control when deflected in identical direction and for roll control when deflected in opposite direction; control organs 1, 3 are used for yaw control when deflected in identical direction and for roll control when deflected in opposite direction. This is the case for maneuverable ballistic missile. Then the control distributions on roll, yaw, and pitch can be presented as follows:

$$\begin{cases} \delta_{\mathrm{r}} = [(\delta_3 - \delta_1) + (\delta_4 - \delta_2)]/4 \\ \delta_{\mathrm{y}} = (\delta_1 + \delta_3)/2 \\ \delta_{\mathrm{p}} = (\delta_2 + \delta_4)/2 \end{cases} \tag{1}$$

with the following additional restriction:

$$\delta_3 - \delta_1 = \delta_4 - \delta_2 \tag{2}$$

By ignoring the higher order terms, the three differential equations which describe the missile pitch plane dynamics (longitudinal perturbations) can be obtained as follows [10-11]:

$$\begin{cases} \Delta\dot{V}_x + a_{10}\Delta V_x + a_{11}\Delta\alpha + a_{12}\Delta\theta = a_{13}\Delta\delta_{\mathrm{p}} \\ \Delta\dot{\theta} + a_{20}\Delta V_y + a_{21}\Delta\alpha + a_{22}\Delta\theta = a_{23}\Delta\delta_{\mathrm{p}} \\ \Delta\ddot{\theta} + a_{30}\Delta V_z + \Delta\ddot{\alpha} + a_{31}\Delta\dot{\alpha} + a_{32}\Delta\alpha + a_{31}\Delta\dot{\theta} = a_{34}\Delta\delta_{\mathrm{p}} \end{cases} \tag{3}$$

where "Δ" describe the perturbations in the dynamics equations.

Replace $\Delta\theta$ and $\Delta\dot{\theta}$ in Eq. (3) using following relations:

$$\begin{cases} \Delta\theta = \Delta\vartheta - \Delta\alpha \\ \Delta\dot{\theta} = \Delta\dot{\vartheta} - \Delta\dot{\alpha} \end{cases}$$

Then taking Laplace transform for the yielded equation, we get

$$\begin{bmatrix} -s + (a_{21} - a_{22}) & s + a_{22} \\ a_{32} & s^2 + a_{31}s \end{bmatrix} \begin{bmatrix} \Delta\alpha \\ \Delta\vartheta \end{bmatrix} = \begin{bmatrix} a_{23} \\ a_{34} \end{bmatrix} \Delta\delta_{\mathrm{p}} \tag{4}$$

The solution of this matrix equation is given by

$$\begin{bmatrix} \Delta\alpha \\ \Delta\vartheta \end{bmatrix} = \frac{1}{\Lambda} \begin{bmatrix} s^2 + a_{31}s & -s - a_{22} \\ -a_{32} & -s + (a_{21} - a_{22}) \end{bmatrix} \begin{bmatrix} a_{23} \\ a_{34} \end{bmatrix} \Delta\delta_{\mathrm{p}} \tag{5}$$

where Λ is matrix determinant, and

$$\begin{cases} a_{21} = \dfrac{1}{mV_{\mathrm{M}}} \left[c_{x_{\mathrm{ru}}} q_{\mathrm{ru}} S_{\mathrm{ru}} - P_{y_{\mathrm{thr}}} - \dfrac{1}{2}\rho V_{\mathrm{M}}^2 S_{\mathrm{M}} c_y^{\alpha} \right] \\ a_{22} = \dfrac{-g}{V_{\mathrm{M}}} \sin\theta \\ a_{23} = \dfrac{2c_{y_{\mathrm{ru}}}^{\delta}}{mV_{\mathrm{M}}} q_{\mathrm{ru}} S_{\mathrm{ru}} \\ a_{24} = \dfrac{1}{mV_{\mathrm{M}}} \\ a_{31} = \dfrac{-\rho V_{\mathrm{M}} S_{\mathrm{M}} D_{\mathrm{M}}}{I_Z} (A_Z^{wz} x_{\mathrm{cg}}^2 + B_Z^{wz} x_{\mathrm{cg}} + C_Z^{wz}) \\ a_{32} = \dfrac{-S_{\mathrm{M}} \rho V_{\mathrm{M}} c_y^{\alpha}}{I_Z} (x_{\mathrm{cg}} - x_{\mathrm{cp}}) \\ a_{34} = \dfrac{2c_{y_{\mathrm{ru}}}^{\delta} q_{\mathrm{ru}} S_{\mathrm{ru}}}{I_Z} (x_{\mathrm{rud}} - x_{\mathrm{cg}}) \end{cases} \tag{6}$$

where q_{ru} is the rudder dynamic pressure, N/m^2; D_{M} the missile diameter, m; I_Z the pitch moment of inertia, kg·m^2; ρ the air density, kg/m^3; $c_{x\mathrm{ru}}$ the rudder drag coefficient in χ_e axis. c_y^{α} the induced lift force coefficient due to angle of attack; $c_{y_{\mathrm{ru}}}^{\delta}$ the lift- drag ratio coefficient and $c_{y_{\mathrm{ru}}}^{\delta} = \partial c_{y_{\mathrm{ru}}} / \partial\delta > 0$ for one rudder; $P_{y_{\mathrm{thr}}}$ the thrust force in y_{e} axis; A_Z^{wz}, B_Z^{wz}, and C_Z^{wz} are coefficients of missile angular velocity ω around z_{e} axis as a function in x_{cg}; S_{M} and S_{ru} the missile and rudder cross sectional area, m^2; the lengths x_{cg}, x_{cp}, and x_{rud} can be defined as shown in Fig. 2.

Then, the transfer function of the missile dynamics in pitch plane is obtained:

$$w_{\delta}^{\vartheta}(s) = \frac{\Delta\vartheta(s)}{\Delta\delta_{\mathrm{p}}(s)} = \frac{k_{\delta}^{\vartheta}(1 + T_0 s)}{(T_2^2 s^2 + 2\xi T_2 s + 1)(\tau s + 1)} \tag{7}$$

where

$$\begin{cases} k_{\delta}^{\vartheta} = a_{34}(a_{21} - a_{22}) - a_{23}a_{32} \\ T_0 = \dfrac{-a_{34}}{a_{34}(a_{21} - a_{22}) - a_{23}a_{32}} \\ T_2 = \dfrac{1}{\sqrt{a_{32} + a_{31}(a_{21} - a_{22})}} \\ \tau = \dfrac{a_{32} + a_{31}(a_{21} - a_{22})}{-a_{32}a_{22}} \\ \xi = \dfrac{a_{21} - a_{22} + a_{31}}{2} T_2 \end{cases} \tag{8}$$

The standard missile flight conditions for dynamic analysis are shown in Table 1. The missile pitch plane dynamic parameters at selected flight time instants are shown in Table 2. Fig. 3 demonstrates the frequency

response of the missile pitch plane dynamic at different flight time instants. It can be seen that the missile is aerodynamically unstable.

Table 1 Flight conditions for dynamic analysis at selected flight time instants

Flight time instant/s	Mach number *Ma*	Velocity/(m·s^{-1})	Altitude/km	Angle of attack/(°)
1	0.013	4.560	0.001 0	0
10	0.350	118.488	0.536 5	−5.100
20	0.830	273.400	2.336 0	−0.045
30	1.400	444.150	5.425 0	0.355
40	2.200	654.790	9.795 0	−0.284
50	3.180	945.350	15.647 0	−0.136
60	4.530	1 345.700	10.749 0	1.770

Table 2 Missile pith dynamic parameters

Flight time instant/s	k_δ^ϑ	T_0	T_2	τ	ξ
1	64.711	1.884 0	2.520	−7.745	0.873
10	3.730	6.386 0	0.812	−14.423	0.163
30	2.960	4.819 0	0.321	−58.570	0.092
50	1 203.770	8.143 5	3.886	−200.607	0.499
60	77.507	15.892	1.181	−237.852	0.069

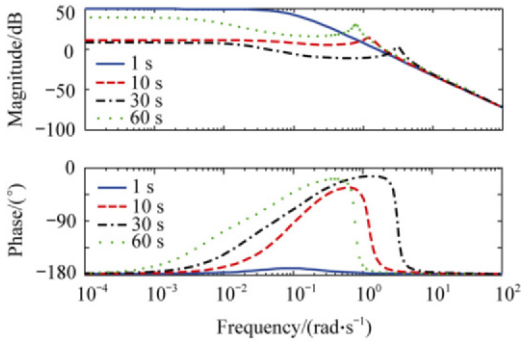

Fig. 3 Frequency response of missile pitch dynamic at different flight time instants.

2.2. Actuation system dynamics

The type of actuation system in this model is electric-hydraulic actuator which is represented by four rudders including DC-motor, amplifier, piston and feedback based on the system requirements which are chosen as maximum deflection angle 5°, maximum hinge moment 40 kg·m, and the band-width 20 Hz [1,11-13]. The transfer function of actuation system design can be written as

$$w_{\mathrm{Ac}}(s)=\frac{K_{\mathrm{di}}K_{\mathrm{c}}K_{\mathrm{g}}}{s(T_{\mathrm{c}}s+1)(T_{\mathrm{d}}s+1)+K_{\mathrm{di}}K_{\mathrm{c}}K_{\mathrm{g}}} \tag{9}$$

where K_{di} is the angle to current ratio, mA/(°); K_{c} the gain of amplifier unit; K_{g} the power gain of servo mechanism, kg/mA; T_{c} the time constant of amplifier unit, s; T_{d} the delay time of servo mechanism, s.

Table 3 shows the main characteristics of the actuation system. Fig. 4 shows closed-loop step response and maximum hinge moment of the actuation system.

Table 3 Actuator characteristics

Parameter	Value
Natural frequency/(rad·s^{-1})	29.580
Overshoot/%	0.706
Settling time/s	0.160
Time constant/s	0.058
Damping ratio	0.844
Damping frequency/(rad·s^{-1})	15.860
Delay time/s	0.020

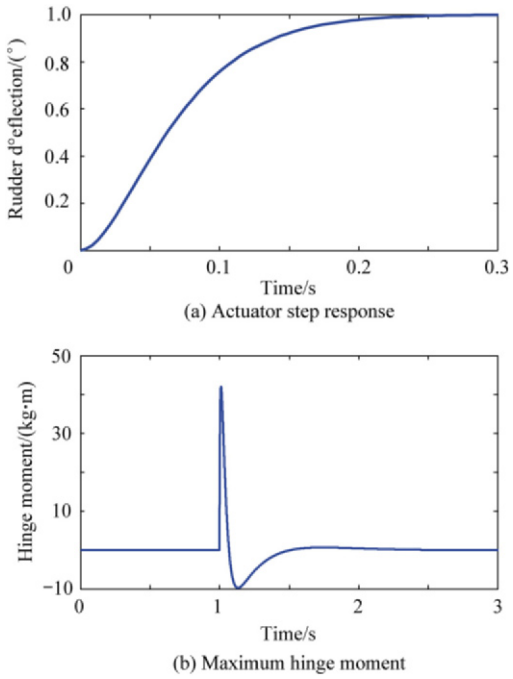

Fig. 4 Actuator step response and maximum hinge moment.

2.3. Modeling of current longitudinal autopilot

Longitudinal autopilot ("pitch channel") of the ballistic missile can be examined separately from the other channels of yaw and roll because the deflection of the practical angle coordinates ϑ, ψ and φ is so small that interference between channels is eliminable when the autopilot system works correctly.

Pitch channel autopilot consists of a pitch compensator, an east gyro which can measure pitch angle and produce program command signals of the pitch angle, and a servomechanism system. Fig. 5 shows autopilot pitch channel model. The control system is designed to perform a specific task such that the performance specifications are satisfied. These specifications are generally related to accuracy, stability and speed of response [14]. The existing longitudinal autopilot employs time-invariant passive-RLC network compensa-

tor as a control strategy, which does not take into account the time-varying missile dynamics. Fig. 6 shows passive-RLC compensator network, where ϑ_{prog} is programmed pitch angle, δ and δ_c are actual and commanded rudder deflection angles respectively, (°).

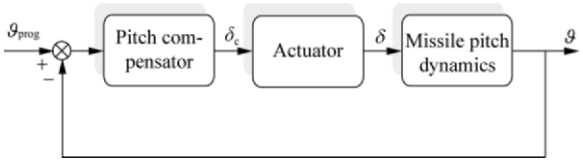

Fig. 5 Autopilot pitch channel model.

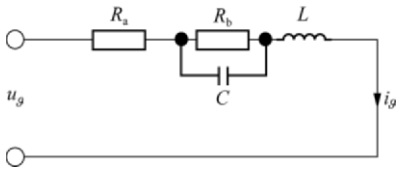

Fig. 6 Passive-RLC compensator network.

The compensation network's Laplace-domain transfer function is given by

$$w_{\vartheta}^{\delta}(s) = K_{\text{pc}} \frac{T_{\text{cp}} s + 1}{a_1 s^2 + a_2 s + 1} \tag{10}$$

where $K_{\text{pc}} = 1/(R_a + R_b)$, mA/V; $a_1 = CLR_b/(R_a + R_b)$, s^2; $a_2 = (L + CR_aR_b)/(R_a + R_b)$, s; and $T_{\text{cp}} = R_bC$, s.

The pitch channel autopilot response in presence of different dynamic uncertainty percentages can be shown in Fig. 7. The previous analysis of the current longitudinal autopilot demonstrates that, there is scope for improvement of the current attitude control system. The current system suffers from long settling time, high overshoot, and oscillatory response in presence of dynamic uncertainty.

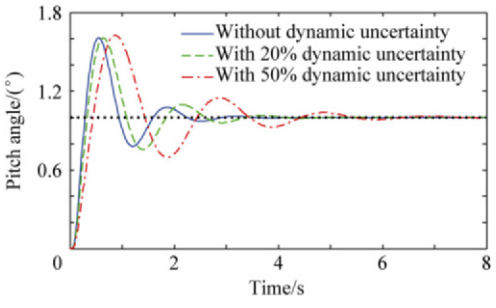

Fig. 7 Pitch autopilot response in presence of dynamic uncertainty with flight conditions: flight time instant=5 s, α=2.000°, and Ma=0.15.

Stability of linear longitudinal autopilot is analyzed by logarithmic frequency characteristic of the open-loop system and step time response of closed-loop system. Table 4 shows the pitch channel characteristics of the current autopilot at different flight time instants.

Table 4 Pitch channel characteristics

Flight time instant/s	Gain margin/dB	Phase margin/(°)	Corner frequency/(rad·s^{-1})
1	12.70	25.1	5.22
10	12.70	27.2	5.43
30	12.10	29.9	6.55
60	9.75	25.4	6.37
Flight time instant/s	**Settling time/s**	**Over shoot/%**	**Rise time/s**
1	2.69	60.7	0.161
10	12.60	43.8	0.171
30	27.80	12.9	0.310
60	3.00	60.8	0.119

3. Research and Development of Improved Attitude Controller

Gain-scheduling is one of the most popular methods for applying LTI control law to time-varying and/or nonlinear systems. In this section two kinds of gain-scheduling controllers are designed for the longitudinal autopilot:

(1) Gain-scheduled optimal tuning-PID with actuator constraints.

(2) Gain-scheduled optimal LQ in conjunction with optimal tuning-compensator.

The proposed controller design methods are pointed out, through their comparison to the current controller of the existence system, which are provided in the MATLAB demo for the autopilot exposed to external disturbances and dynamic uncertainty.

3.1. Design of optimal tuning-PID controller with actuator constraints

The optimal tuning-PID controller with actuator constrains is designed in MATLAB environment using Simulink response optimization software which is called the nonlinear control design (NCD) blockset. This software has features include the ability to optimize design criteria in any Simulink model by tuning selected model parameters that include physical actuation limits. Using Simulink response optimization, one can easily factor in design requirements expressed in terms of rise time, settling time, overshoot, and saturation limits. The steepest descent optimization method is chosen to find the optimal tuning-PID gains. The method of the steepest descent, also known as the gradient descent, is the simplest one of the gradient methods [15].

A PID regulator is designed with actuator constraints so that deflection response of actuator and closed-loop system can meet the following constraints for tracking:

(1) Rudder maximum deflection angle: ±5°.

(2) Maximum oscillation: 20%.

(3) Maximum rise-time: 0.5 s.

(4) Maximum overshoot: 10%.

(5) Maximum time-response: 1 s.

The designed Simulink model containing optimal tuning application and control structure is shown in Fig. 8. An input step drives the system. NCD blocks are attached to blocks of actuator and missile dynamics in order to connect the signals, which will be restricted. Tunable and uncertain variables are initialized. The uncertain variables of missile dynamics are initialized at nominal values. Tunable parameters K_p (proportional gain), K_i (integral gain) and K_d (derivative gain) are initialized at 0.632 3, 0.049 3, and 2.027 2 respectively. These values result from the use of Ziegler-Nichols method for PID regulators [16].

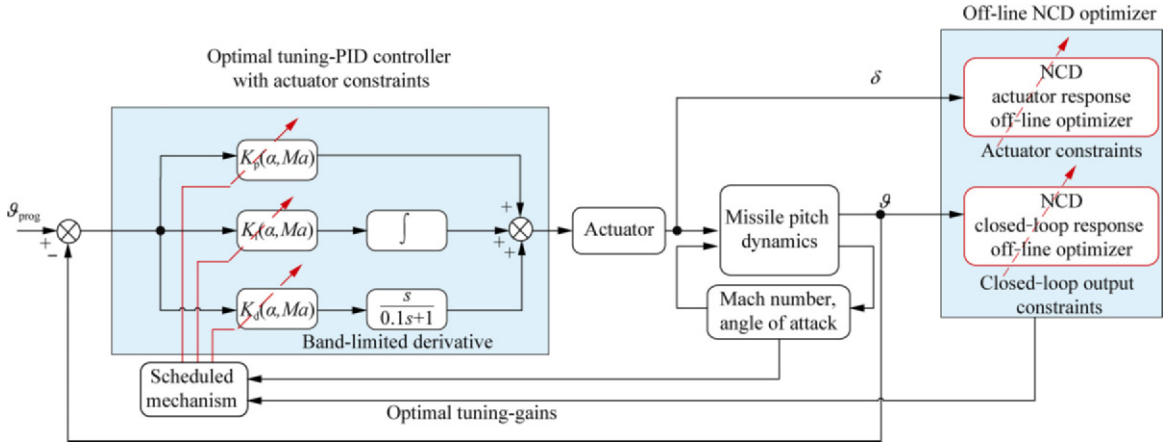

Fig. 8 Pitch channel with optimal tuning-PID controller design structure.

The Ziegler-Nichols tuning method is a heuristic method of tuning a PID controller. It is performed by setting the K_i and K_d to zero. K_p is then increased (from zero) until it reaches the ultimate gain K_u, at which the output of the control loop oscillates with a constant amplitude. K_u and the oscillation period T_u are used to set the PID controller gains depending on the type of controller used. Table 5 demonstrates Ziegler-Nichols method.

Table 5 Ziegler-Nichols method

Control type	K_p	K_i	K_d
P	$K_u/2$	—	—
PI	$K_u/2.2$	$1.2K_p/T_u$	—
Classic PID	$0.6K_u$	$2K_p/T_u$	$K_pT_u/8$
Pessen integral rule	$0.7K_u$	$2.5K_p/T_u$	$0.15K_pT_u$

Then, the limitations of time are defined. Upper and lower restriction limits define oscillation, rise time, response time, and actuator constraints. After running optimization, the time, the cost function evolution and the final values for tunable parameters vary depending on computer's performance [17-18]. Fig. 9 shows the iterative steps of the optimization process for actuator response and closed-loop system. In Fig. 9, it can be seen there are two background colors, where the white color indicate the selected design constraints. Moreover, the black line is used to plot the optimized response of the final iterative step.

The entire design optimization process is repeated for other flight conditions of boost phase flight instants. The set of control gains is then formed into the data set for the gain schedule.

In Ref. [1], a second order polynomial function was fit to the data points for each state every step in real-time flight. Fig. 10 shows the scheduled gains of the optimal tuning-PID controller.

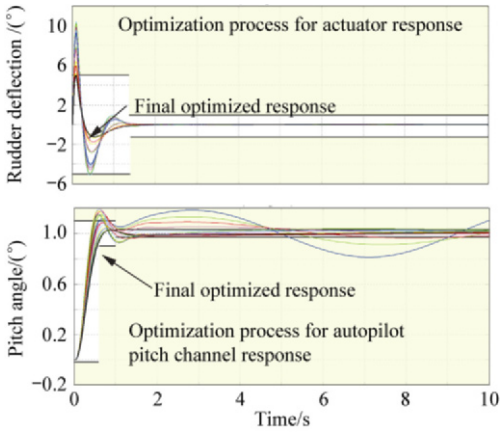

Fig. 9 Iterative steps of optimization process for actuator response and closed-loop system with flight conditions: flight time instant is 5 s, and Ma=0.15.

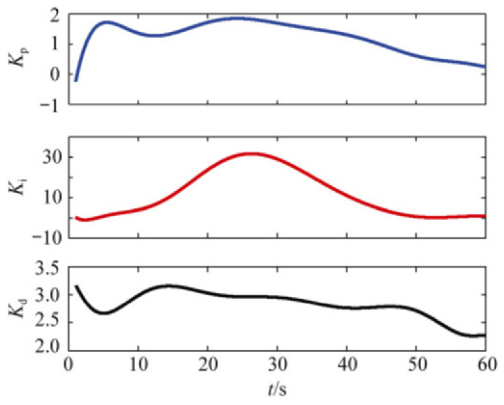

Fig. 10 Scheduled PID gains K_p, K_i, and K_d.

3.2. Design of optimal LQ controller with optimum tuning-compensator

The LQR requires full state feedback, including body pitch angle rate and angle of attack, which are currently not transduced. There are known performance and robustness advantages in using full state feedback, however estimation of system states is necessary in this case. The introduction of a three-axis body rate sensor solves the body rate estimation problem discussed later. The advantages of full state feedback include two aspects:

(1) Weighted quadratic cost function can be minimized.

(2) It could be gain-scheduled.

The pure optimal control method LQR/LQG with full state feedback including actuator dynamics fails to improve the attitude stability. The LQG regulator with full state feedback is modified without taking into account the actuator dynamics. The linear quadratic optimal control techniques are considered including LQR optimal regulator and reduced order state estimator in conjunction with optimal tuning-compensator. The designed controller structure is shown in Fig. 11, where K_{LQR} is the optimal LQR gain matrix, δ_{dmd} actuator command input, L_{r} Kalman gain, $\hat{\boldsymbol{x}}$ estimated states matrix, ϑ_{FB} ouput feedback.

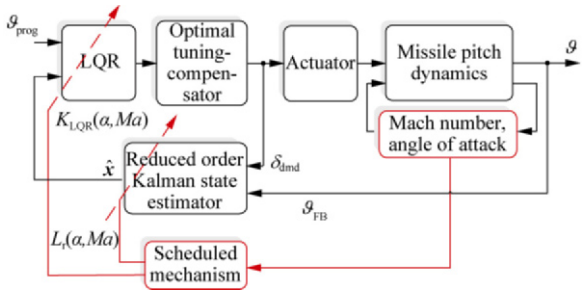

Fig. 11 Designed structure of reduced order LQG in conjunction with optimal tuning-compensator.

A given missile pitch dynamics system is represented as follows:

$$\dot{\boldsymbol{x}} = \boldsymbol{A}(\alpha, Ma)\boldsymbol{x} + \boldsymbol{B}(\alpha, Ma)u \tag{11}$$

where

$$\boldsymbol{A}(\alpha, Ma) = \begin{bmatrix} -a_{31}(\alpha,Ma) & 0 & -a_{31}(\alpha,Ma) \\ 1 & 0 & 0 \\ 1 & a_{22}(\alpha,Ma) & a_{21}(\alpha,Ma)-a_{22}(\alpha,Ma) \end{bmatrix}$$

$$\boldsymbol{x} = \begin{bmatrix} \Delta\dot{\vartheta} \\ \Delta\vartheta \\ \Delta\alpha \end{bmatrix}, \quad \boldsymbol{B}(\alpha, Ma) = \begin{bmatrix} a_{34}(\alpha,Ma) \\ 0 \\ -a_{23}(\alpha,Ma) \end{bmatrix}, \quad u = \delta_{\mathrm{p}}$$

Then determine the optimal feedback gains matrix $\boldsymbol{K}$ of the LQR such that $\boldsymbol{u}(t)=-\boldsymbol{K}\boldsymbol{x}(t)$ to minimize the following performance index:

$$J_{\mathrm{LQR}}(\boldsymbol{u}) = \frac{1}{2}\int_0^{t_{\mathrm{f}}} \boldsymbol{x}^{\mathrm{T}}(t)\boldsymbol{Q}\boldsymbol{x}(t) + \boldsymbol{u}^{\mathrm{T}}(t)\boldsymbol{R}\boldsymbol{u}(t)\mathrm{d}t \tag{12}$$

where $\boldsymbol{Q}$ and $\boldsymbol{R}$ are the positive-definite Hermitian or real symmetric matrix. A reasonable simple choice for matrices $\boldsymbol{Q}$ and $\boldsymbol{R}$ is given by Bryson's rule by selecting $\boldsymbol{Q}$ and $\boldsymbol{R}$ to be diagonal with $Q_{ii}=1/x_{i,\max}^2$, $R_{jj}=1/u_{j,\max}^2$, where $x_{i,\max}^2$ is the maximum acceptable value of x_i^2 and $u_{i,\max}^2$ the maximum acceptable value of u_i^2. The LQR weightings are chosen in an attempt to recover properties of the existing system, while maintaining stability over an increased angular range. By selecting a high state weighting $\boldsymbol{Q}$, the system is forced to minimize tracking error, which is desirable. The body rates being driven to zero should not be penalized, because that slows the vehicle response. The control weightings are minimized to improve vehicle response, while avoiding actuator saturation. The state weighting on pitch error is higher than that in other states. It is desirable to keep the pointing loop tightly controlled. Matrices $\boldsymbol{Q}$ and $\boldsymbol{R}$ are chosen as follows:

$$\boldsymbol{Q} = \begin{bmatrix} 0 & 0 & 0 \\ 0 & 3\times10^5 & 0 \\ 0 & 0 & 1\times10^2 \end{bmatrix}, \quad R = 3 \tag{13}$$

The state feedback gain $\boldsymbol{K}$ is also found by minimizing the linear quadratic cost function, by solving the continuous algebraic Ricatti equation. It can be derived from $\boldsymbol{P}$ by the following equation:

$$\boldsymbol{K} = \boldsymbol{R}^{-1}\boldsymbol{B}^{\mathrm{T}}\boldsymbol{P} \tag{14}$$

where $\boldsymbol{P} \geqslant \boldsymbol{0}$ is the maximal stabilizing solution to the following continuous algebraic Ricatti equation:

$$\boldsymbol{A}^{\mathrm{T}}\boldsymbol{P} + \boldsymbol{P}\boldsymbol{A} + \boldsymbol{Q} - \boldsymbol{P}\boldsymbol{B}\boldsymbol{R}^{-1}\boldsymbol{B}^{\mathrm{T}}\boldsymbol{P} = \boldsymbol{0} \tag{15}$$

The Ricatti equation is solved by using MATLAB lqr(A, B, C, D) for each flight conditions of boost phase flight instants in order to form the gain-scheduling of optimal state feedback gains, as in Fig. 12, where K_{x1}, K_{x2}, and K_{x3} are scheduled LQR gains.

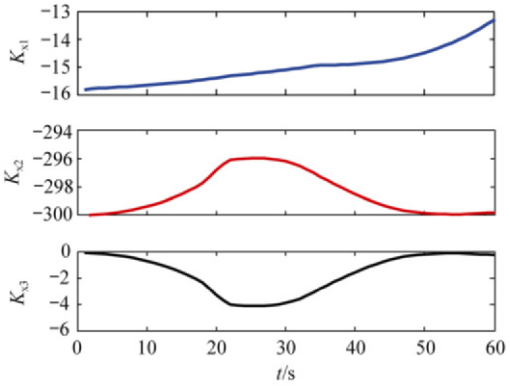

Fig. 12 Scheduled LQR gains K_{x1}, K_{x2}, and K_{x3}.

The dynamics of optimal LQ regulator with state estimator is given:

$$\begin{cases}\dot{\hat{x}} = [A - L_r C - (B - L_r D)K]\hat{x} + L_r y \\ u = -K\hat{x}\end{cases} \quad (16)$$

The state estimator is designed using MATLAB facility with state noise weight Q_N=1 and control noise weight R_N=1. The control input part of the filter gain is neglected as the estimator is implemented in reduced order. Fig. 13 shows the design of the reduced order estimators with Kalman gain L_r.

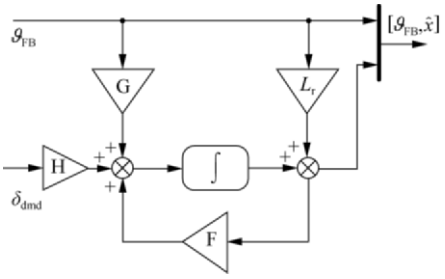

Fig. 13 Reduced order estimators with Kalman gain L_r.

Although the noise weights have a physical significance, they are used to tune the controller response. High weights are placed on the state and control error, to simulate high plant uncertainty. The Kalman gain found above is implemented in a reduced order estimator, to obtain more accurate feedback measurements. The system is partitioned between measured and estimated states. The optimal reduced order estimator gain L_r is selected from the Kalman gain. Low gains are desirable due to gyroscope sensor error, which will lead to poor estimates if the plant output is amplified. The lower limit on the gains as the noise weights are increased is unity I.

The controller is constructed in Simulink, and modeled with the linearized vehicle, actuator and gyroscope sensor. It is found that the response is inadequate, and compensators are required for neglected actuator dynamics. The existing compensators are introduced after retuning by gradient descent optimization method applying Simulink response optimization software NCD, which is introduced before. After tuning of the compensator, the vehicle response is deemed acceptable. The response is presented and compared with the existing control system. Small but insignificant improvements to the attitude envelope are achieved with the optimal LQ gain and reduced order estimator. The reduced order LQG is more divergently unstable than the existing controller, when dynamic uncertainty is induced.

Finally the design is modified to achieve the LQR robustness. The robust hybrid control is obtained by designing reduced order LQR in conjunction with optimal tuning-compensator. The reduced order LQR problem is solved without taking into account the actuator dynamics. Moreover, the gain-scheduled is considered for two-state feedback by ignoring angle of attack state feedback which has less dynamic effect. The proposed longitudinal controller offers the greatest scope for controller improvement, and guarantees $\zeta >$ 0.7 with overshoot <10% in the presence of dynamic uncertainty and large disturbance. This approach is tested through various scenarios for the validated nonlinear dynamic flight model of the real ballistic missile system with autopilot exposed to external disturbances. The modified control design of reduced order LQR in conjunction with optimal tuning-compensator is shown in Fig. 14.

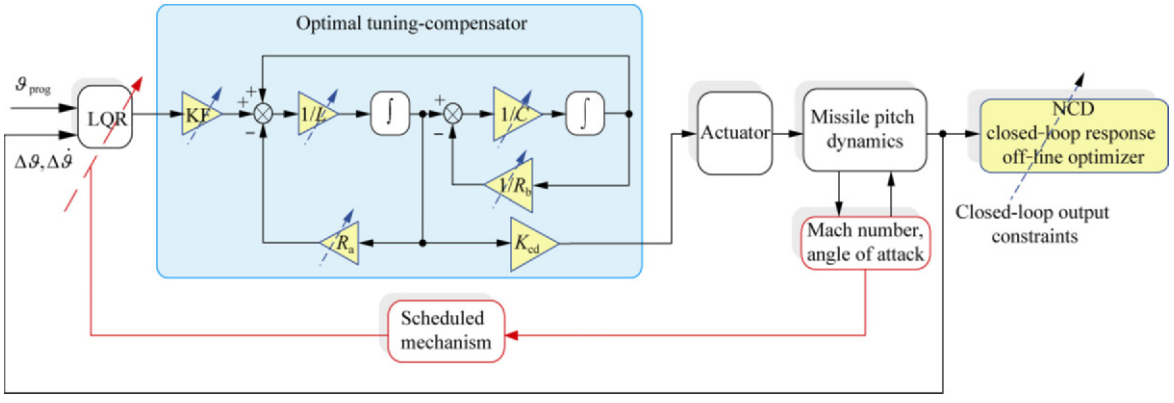

Fig. 14 Modified designed structure of reduced order LQR in conjunction with optimal tuning-compensator.

4. Simulation and Comparisons

4.1. Longitudinal autopilot closed-loop characteristics in nominal case

Figs. 15-17 demonstrate that the gain-scheduled optimal LQR with tuning-compensator has the optimum performance: fast response, the smallest overshoot and the shortest settling time.

4.2. Longitudinal autopilot closed-loop characteristics in presence of dynamic uncertainty

The proposed gain-scheduled controllers are tested

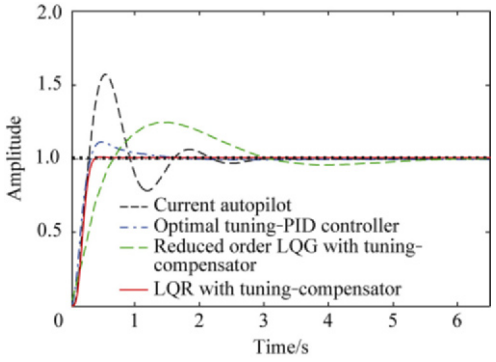

Fig. 15 Response of designed controllers with flight conditions: flight time instant is 5 s, α=2.000°, and Ma=0.15.

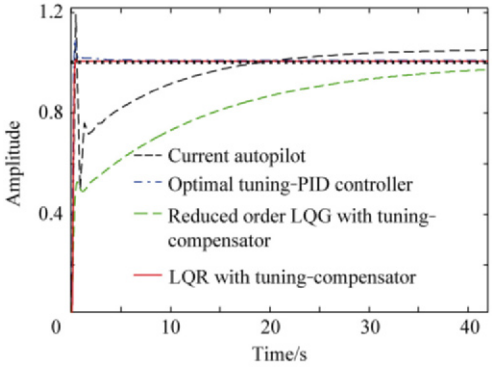

Fig. 16 Response of designed controllers with flight conditions: flight time instant is 30 s, α=0.355°, and Ma=1.4.

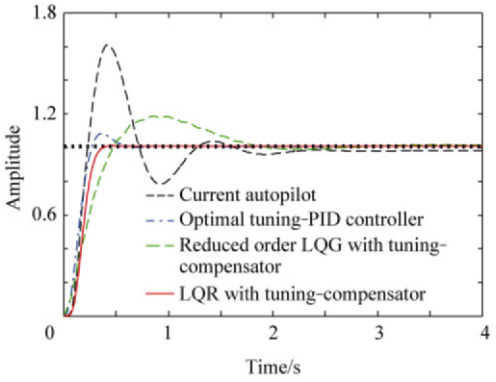

Fig. 17 Response of designed controllers with flight conditions: flight time instant is 60 s, α=−0.200°, and Ma=2.2.

under severe dynamic uncertainty. The parametric uncertainties are changed due to a change in aerodynamic coefficients given as follows:

$$\begin{cases} a'_{21}(\alpha,Ma)=1.2a_{21}(\alpha,Ma) \\ a'_{22}(\alpha,Ma)=1.5a_{22}(\alpha,Ma) \\ a'_{23}(\alpha,Ma)=1.7a_{23}(\alpha,Ma) \\ a'_{31}(\alpha,Ma)=0.7a_{31}(\alpha,Ma) \\ a'_{34}(\alpha,Ma)=0.8a_{34}(\alpha,Ma) \end{cases}$$

The system output is shown in Figs. 18-20 with different flight conditions. We can see that, the gain-scheduled LQR with tuning-compensator still has uniform performance and is more robust than gain-scheduled optimal tuning-PID controller. On the other hand the reduced order LQG and current controllers fail to make the system stable in the presence of system uncertainties and external disturbances. Finally, through the analytical results of previously proposed controllers, the gain-scheduled LQR in conjunction with optimal tuning-compensator is proposed to achieve the fully boost phase flight control for the ballistic missile.

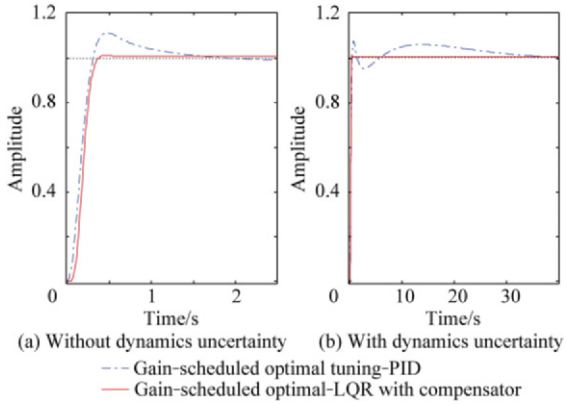

Fig. 18 Response of gain-scheduled controllers in the presence of dynamic uncertainty with flight conditions: flight time instant is 5 s, α=2.000°, and Ma=0.15.

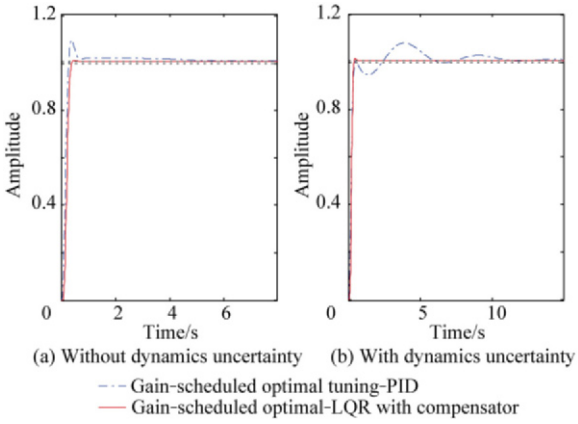

Fig. 19 Response of gain-scheduled controllers in the presence of dynamic uncertainty with flight conditions: flight time instant is 10 s, α=−5.000°, and Ma=0.35.

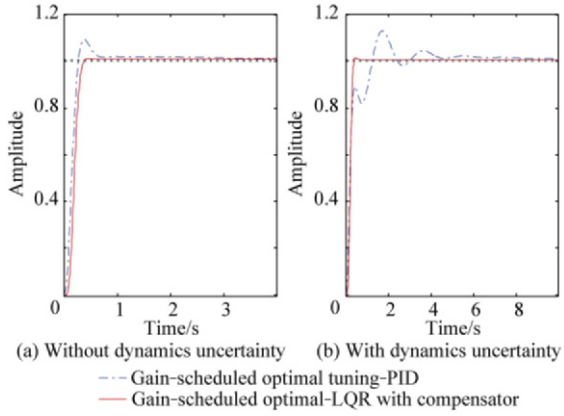

Fig. 20 Response of gain-scheduled controllers in the presence of dynamic uncertainty with flight conditions: flight time instant is 30 s, α=0.355°, and Ma=1.4.

4.3. Longitudinal autopilot performance with dynamic flight simulation

For investigating the performance of the developed longitudinal autopilot with the proposed controller and keeping with the requirements for a continued development, the full dynamic simulation is established for ballistic missile equipped by thrust vector control system. The mathematical model is structured as a series of modules. These modules can be individually developed, for instance, airframe structure module, range control module, pitch program module, thrust variation module, weight data module, variation of missile mass center module, variation of mass center of oxidizer and fuel tanks for liquid rocket motor, gravity module, earth module, variation of inertial moment module, and atmospheric data module [11,20-23]. The simulation of the underlying system is carried out on MATLAB environment using the numerical integration method "Runge-Kutta". Sampling time of the trajectory is chosen as 0.01 s. The results are validated against real data and thus can be used for subsequent analysis. The flight scenarios are done for limited range 250 km due to the limitation of the available dynamic data. The simulation studies are performed to validate the designed gain-scheduled LQR in conjunction with tuning-compensator controller using a priori known implicit guidance scheme for typical ballistic missile trajectory. The plant model used in the simulations includes the actuator dynamics. The output rudder deflection is limited, but this limit has never been approached during simulation. The parametric variations of the system's transfer function are caused by changes in aerodynamic coefficients.

Different flight simulation scenarios are run to investigate the developed longitudinal autopilot.

Scenario 1: Nominal trajectory condition without dynamic uncertainty. Figs. 21-23 demonstrate trajectory, total velocity, angle of attack α, missile pitch response ϑ, and rudder deflection in pitch plane δ_p. The results demonstrate the succession of both the current

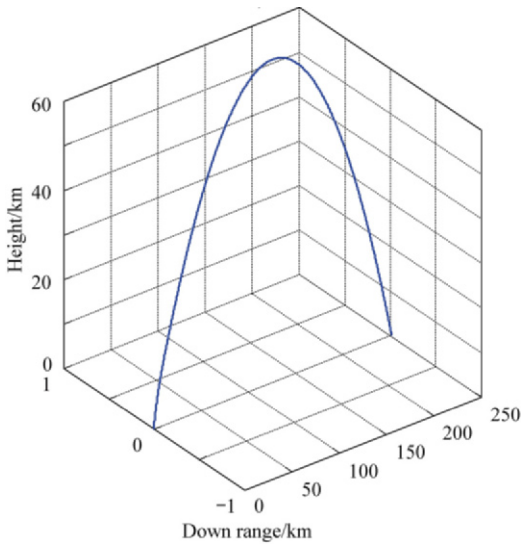

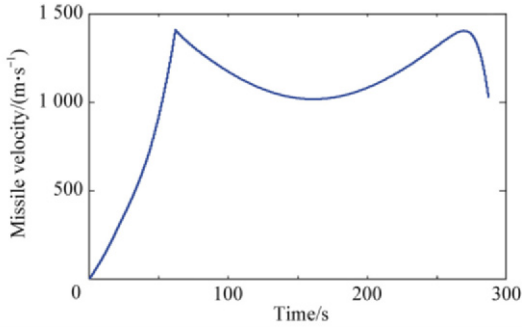

Fig. 21 Nominal trajectory and missile velocity with the developed autopilot (Scenario 1).

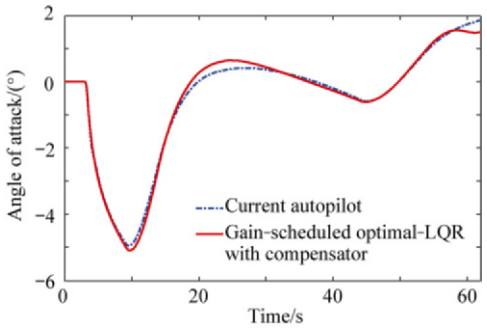

Fig. 22 Angle of attack of nominal trajectory (Scenario 1).

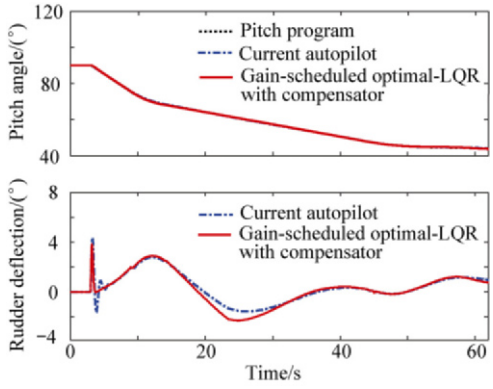

Fig. 23 Missile pitch angle ϑ response and rudder deflection δ_p for nominal flight conditions (Scenario 1).

and developed autopilots to steer the missile to a shut-off point at the same flight time instance and hit the target with the same trajectories. It can be seen from Fig. 23 that the developed autopilot has much better rudder angle time response (lower overshoot with no backward peak) compared with the current autopilot.

Scenario 2: Launch with initial pitch angle error as 1° without adding dynamic uncertainty. Fig. 24 demonstrates the missile behavior and rudder deflection response against the initial pitch angle error.

Scenario 3: Induced wind disturbances in pitch plane during flight period time [10, 15] s with wind speed 10 m/s without adding dynamic uncertainty. Fig. 25 shows the robustness of the developed autopilot compared with the current autopilot in the presence of wind disturbance.

Scenario 4: Induced wind disturbances in pitch plane during period time [15, 18] s with wind speed 20 m/s in the presence of 30% dynamic uncertainty. Fig. 26 demonstrates the results. It can be seen that the missile equipped by the developed longitudinal autopilot damps the wind disturbance and reruns to the reference pitch profile. On the other hand, the missile equipped with current autopilot gets a large flight path deviation, affected by dynamic uncertainty and wind disturbance.

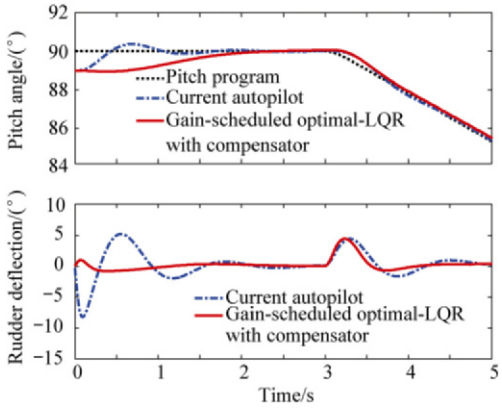

Fig. 24 Missile behavior and rudder deflection response against intial pitch error (Scenario 2).

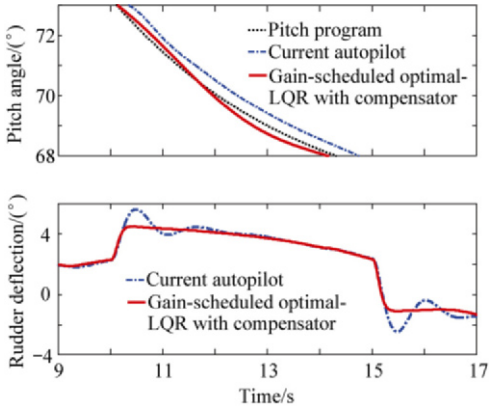

Fig. 25 Induced wind disturbances in pitch plane during period time [10, 15] s with wind speed 10 m/s without dynamic uncertainty (Scenario 3).

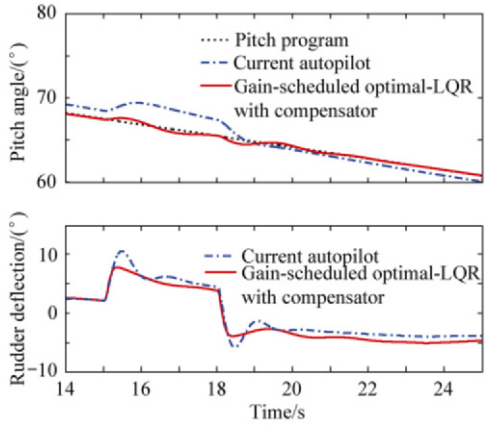

Fig. 26 Missile response against induced wind disturbances in pitch plane during period time [15, 18] s with wind speed 20 m/s including 30% dynamic uncertainty (Scenario 4).

It can therefore be concluded that developed gain-scheduled LQR in conjunction with tuning-compensator exhibits excellent robustness characteristics to modeling uncertainty and presence of wind disturbances.

5. Conclusions

(1) The employing of time-invariant passive-RLC network compensator as a control strategy may cause the closed-loop system instability in the presence of large disturbance and dynamics uncertainty.

(2) Gain-scheduled optimal tuning-PID with actuator constraints, supplies better response but requires a priori knowledge of the system dynamics. Moreover, the controller has oscillatory response in the presence of dynamic uncertainty.

(3) From the point of view of reliable flight control systems design, the purely optimal control design methodologies based on the LQR has good stability properties, but may be sensitive to off-nominal conditions. Moreover, the implementation requires all state variables as feedback, some of which however cannot be easily measured. If an observer is used to reconstruct the state vector from available measurements, then the optimal control system often has much less satisfactory stability property, and the system performance is very much affected by parameter variations as will as satisfactory disturbances.

(4) The robust hybrid control is obtained by designing reduced order LQR in conjunction with optimal tuning-compensator.

(5) The use of rate gyro is recommended to solve the optimal LQR regulator requirements.

(6) The proposed longitudinal controller is tested through various scenarios for the validated nonlinear dynamic flight model of the real ballistic missile system with autopilot exposed to external disturbances. The controller is currently under review.

References

[1] Siouris G M. Missile guidance and control systems. New York: Springer-Verlag, 2004.

[2] Tsourdos A, Hughes E J, White B A. Fuzzy multi-objective design for a lateral missile autopilot. Control Engineering Practice 2006; 14(5): 547-561.

[3] Leith D J, Leithead W E. Survey of gain-scheduling analysis and design. International Journal of Control 2000; 73(11): 1001-1025.

[4] Saussié D, Saydy L, Akhrif O. Gain scheduling control design for a pitch-axis missile autopilot. AIAA Guidance, Navigation and Control Conference and Exhibit. 2008.

[5] Rugh W J, Shamma J S. Research on gain-scheduling. Automatica 2000; 36(10): 1401-1425.

[6] Fromion V, Scorletti G. A theoretical framework for gain scheduling. International Journal of Robust and Nonlinear Control 2003; 13(10): 951-982.

[7] Mehendale C S, Grigoriadis K M. A new approach to

LPV gain-scheduling design and implementation. Proceedings of 43rd IEEE Conference on Decision and Control. 2004.
[8] Wu F, Packard A, Balas G. Systematic gain-scheduling control design: a missile autopilot example. Asian Journal of Control 2002; 4(3): 341-347.
[9] Joseph M F. LQG/LTR optimal attitude control of small flexible spacecraft using free-free boundary conditions. PhD thesis, Aerospace Engineering Sciences Department, University of Colorado, 2006.
[10] Chang C B. Ballistic trajectory estimation with angle-only measurements. IEEE Transactions on Automatic Control 1980; 25(3): 474-480.
[11] Ibrahim I A. Analysis and design of guidance navigation and control system for missile applications. PhD thesis, Navigation Guidance and Control Department, Beihang University, 2004.
[12] He L S. Launch vehicle design. Beijing: Beihang University Press, 2004.
[13] Chen H, Qi X, Chen J, et al. Research on anti-control of missile electro-hydraulic actuator using active disturbance rejection control method. Fourth International Conference on Innovative Computing Information and Control. 2009; 1443-1446.
[14] John H B. Automatic control of aircraft and missiles. 2nd ed. New York: Air Force Institute of Technology, 1991.
[15] Wang X. Method of steepest descent and its applications. <http://sces.phys.utk.edu/~moreo/mm08/Xu WangP571. pdf>. Knoxville, TN: Department of Engineering, University of Tennessee, 2008.
[16] Rasmussen H. Automatic tuning of PID-regulators. < http://www.control.auc.dk/~hr/adapt/auto.pdf >. Aalborg, Denmark: Control Engineering Department, Aalborg University, 2002.
[17] Nonlinear control design blockset, for use with Simulink. Natick, MA: The Math Works, Inc., 2003.
[18] <http://www.mathworks.com/mathematical-modeling/index.html>.
[19] Clement B, Duc G. An interpolation method for gain-scheduling. 40th IEEE Conference on Decision and Control. 2001; 1310-1315.
[20] Dituri J. Ballistic missile trajectory estimation. PhD thesis, Naval Postgraduate School, 2006.
[21] Zarchan P. Tactical and strategic missile guidance. 3rd ed. Washington, D.C.: American Institute of Aeronautics and Astronautics, Inc., 1998.
[22] Sutton G P. Rocket propulsion elements: an introduction to engineering of rockets. 6th ed. New York: John Wiley & Sons, 1992.
[23] Harlin W J, Cicci D A. Ballistic missile trajectory prediction using a state transition matrix. Applied Mathematics and Computation 2007; 188(2): 1832-1847.

Biography:

WAEL Mohsen Ahmed Born in 1973, he received B.S. and M.S. degrees from Military Technical College, Cairo, Egypt in 1996 and 2001 respectively, and then started in 2009 for his Ph.D. degree in Beihang University (BUAA), Beijing, China. His main research interest is missile guidance and control systems.
E-mail: waelsoliman@live.com